Proteoglycan 4: A Dynamic Regulator of Skeletogenesis and Parathyroid Hormone Skeletal Anabolism

Chad M Novince,[1] Megan N Michalski,[1] Amy J Koh,[1] Benjamin P Sinder,[2] Payam Entezami,[1] Matthew R Eber,[1] Glenda J Pettway,[1] Thomas J Rosol,[3] Thomas J Wronski,[4] Ken M Kozloff,[2] and Laurie K McCauley[1,5]

[1]Department of Periodontics and Oral Medicine, School of Dentistry, University of Michigan, Ann Arbor, MI, USA
[2]Department of Orthopaedic Surgery, Medical School, University of Michigan, Ann Arbor, MI, USA
[3]Department of Veterinary Biosciences, College of Veterinary Medicine, The Ohio State University, Columbus, OH, USA
[4]Department of Physiological Sciences, University of Florida, Gainesville, FL, USA
[5]Department of Pathology, Medical School, University of Michigan, Ann Arbor, MI, USA

ABSTRACT

Proteoglycan 4 (*Prg4*), known for its lubricating and protective actions in joints, is a strong candidate regulator of skeletal homeostasis and parathyroid hormone (PTH) anabolism. *Prg4* is a PTH-responsive gene in bone and liver. *Prg4* null mutant mice were used to investigate the impact of proteoglycan 4 on skeletal development, remodeling, and PTH anabolic actions. Young *Prg4* mutant and wild-type mice were administered intermittent PTH(1–34) or vehicle daily from 4 to 21 days. Young *Prg4* mutant mice had decreased growth plate hypertrophic zones, trabecular bone, and serum bone formation markers versus wild-type mice, but responded with a similar anabolic response to PTH. Adult *Prg4* mutant and wild-type mice were administered intermittent PTH(1–34) or vehicle daily from 16 to 22 weeks. Adult *Prg4* mutant mice had decreased trabecular and cortical bone, and blunted PTH-mediated increases in bone mass. Joint range of motion and animal mobility were lower in adult *Prg4* mutant versus wild-type mice. Adult *Prg4* mutant mice had decreased marrow and liver fibroblast growth factor 2 (FGF-2) mRNA and reduced serum FGF-2, which were normalized by PTH. A single dose of PTH decreased the PTH/PTHrP receptor (PPR), and increased *Prg4* and FGF-2 to a similar extent in liver and bone. Proteoglycan 4 supports endochondral bone formation and the attainment of peak trabecular bone mass, and appears to support skeletal homeostasis indirectly by protecting joint function. Bone- and liver-derived FGF-2 likely regulate proteoglycan 4 actions supporting trabeculae formation. Blunted PTH anabolic responses in adult *Prg4* mutant mice are associated with altered biomechanical impact secondary to joint failure. © 2012 American Society for Bone and Mineral Research.

KEY WORDS: PTH; *PRG4*; BONE; LIVER; FGF-2

Introduction

Parathyroid hormone (PTH) has catabolic and anabolic actions in bone, depending on the mode of administration. Continuous PTH administration induces bone resorption, whereas intermittent PTH administration stimulates bone formation.[1] Once-daily teriparatide [PTH(1–34)] injection is currently the only U.S. Food and Drug Administration (FDA)-approved anabolic agent for the treatment of osteoporosis, and is under clinical investigation for the treatment of localized osseous defects.[2,3] Whereas intermittent PTH(1–34) has proven bone forming actions, the mechanisms mediating these anabolic effects are poorly understood.

Osteoblasts and stromal cells are the predominant cells in bone that express the PTH/PTH-related protein (PTHrP) receptor (PPR). PTH signaling in osteoblastic cells has been shown to regulate the expression of growth factors critical for PTH-induced anabolic actions in bone.[4,5] Most notably, PTH anabolic actions have been linked to insulin-like growth factor I (IGF-I) and basic fibroblast growth factor 2 (FGF-2).[6–8] PTH rapidly upregulates FGF-2 mRNA in cultured osteoblastic cells,[4] and intermittent PTH administration increases IGF-I mRNA in bone in vivo.[5] IGF-I and FGF-2 mutant mice have severely blunted to absent anabolic responses to PTH.[6–8]

Proteoglycan 4 (*Prg4*), a novel PTH responsive gene in bone,[9,10] is a strong candidate regulator of the anabolic actions

of PTH. The *Prg4* gene encodes an approximately 345-kD proteoglycan, consisting of 1404 amino acids spanning 12 exons. *Prg4* is expressed in skeletal and nonskeletal tissues, with highest levels of expression in articular joints, bone, and liver.[11,12] The four isolated *Prg4* protein products are secreted glycoproteins, which have been implicated in the protection of articular joints, expansion of hematopoietic progenitor cells, and regulation of megakaryopoiesis. A proteoglycan 4 receptor has not been identified.[12,13]

Loss-of-function mutations in *Prg4* result in the human autosomal recessive disorder camptodactyly–arthropathy–coxa vara–pericarditis (CACP) syndrome, which is primarily characterized by precocious joint failure.[14] Similar to humans presenting with the CACP syndrome, the *Prg4* mutant mouse is afflicted by early onset joint arthropathy.[12] Of interest, osteopenia has been noted in microradiographs of joints from *Prg4* mutant mice.[12] Whereas studies have shown that *Prg4* is endogenously expressed in bone[11] and *Prg4* is a PTH responsive gene in the bone marrow in vivo and isolated osteoblastic cells in vitro,[10] there have been no reported investigations of the actions of proteoglycan 4 in bone. The purpose of this study was to investigate the role of proteoglycan 4 as a regulator of skeletal development, remodeling, and PTH anabolic actions. This investigation of the *Prg4* mutant mouse model provides for the first study of proteoglycan 4 actions in bone.

Materials and Methods

C57BL6 wild-type mice

We harvested long bone (femur and tibia freed of soft tissue), calvaria, bone marrow (flushed from a femur and tibia), and whole liver from untreated 16-week-old C57BL6 wild-type mice for gene expression analyses. In a PTH administration experimental protocol, 8- to 16-week-old C57BL6 wild-type mice were administered a single subcutaneous injection of recombinant human PTH(1–34) (1 μg/g) (Bachem; Torrence, CA, USA) or vehicle (0.9% NaCl), euthanized 1, 4, 8, or 12 hours later, and whole liver, calvaria, and long bone (femur and tibia freed of soft tissue and growth plates sectioned) were harvested for gene expression analyses. All animal studies were approved by the University of Michigan Committee on the Use and Care of Animals (UCUCA), and animals were maintained in accordance with approved UCUCA research protocols.

Prg4 mutant (−/−) mice

Prg4 mutant (−/−) mice, generated by homologous recombination in 129Sv/Ev-derived embryonic stem cells, were generously provided by Matthew Warman (Harvard).[12] *Prg4* −/− mice were backcrossed from the 129Sv/Ev genetic background to the C57BL6 genetic background. We used a PCR-based assay to genotype the mice as previously described.[12]

Sixteen-week-old *Prg4* −/− mice and wild-type (+/+) littermates were administered a single subcutaneous injection of recombinant human PTH(1−34) (1 μg/g) (Bachem) or vehicle (0.9% NaCl), euthanized 0 (no treatment control), 1, 4, 8, or 12 hours later, and bone marrow (flushed from a femur and tibia) and whole liver were harvested for gene expression analyses.

In an intermittent PTH administration experimental protocol, we administered 4-day-old *Prg4* −/− and +/+ littermate mice once-daily subcutaneous injection of recombinant human PTH(1–34) (50 μg/kg) (Bachem) or vehicle (0.9% NaCl) control for 17 days, from day 4 to 21. *Prg4* mice treated from day 4 to 21 are referred to here as "young" *Prg4* mice. In another intermittent PTH administration experimental protocol, we administered 16-week-old *Prg4* −/− and +/+ littermate mice once-daily subcutaneous injection of recombinant human PTH(1–34) (50 μg/kg) (Bachem) or vehicle (0.9% NaCl) control for 6 weeks, from 16 to 22 weeks. *Prg4* mice treated from 16 to 22 weeks are referred to here as "adult" *Prg4* mice. We administered adult *Prg4* mice an intraperitoneal injection of calcein (Sigma-Aldrich, St. Louis, MO, USA) (20 mg/kg), dissolved in calcein buffer (0.15 M NaCl, 2% NaHCO₃), 5 days and 2 days prior to euthanasia. Twenty-four hours following the final PTH injection, we euthanized the mice and harvested their tissues for analyses.

Quantitative real-time PCR

Bone marrow was directly flushed from a femur and tibia with TRIzol reagent (Invitrogen, Carlsbad, CO, USA). Long bone, calvaria, and whole liver were flash frozen, pulverized, and homogenized in TRIzol reagent. Bone marrow stromal cell (BMSC) cultures were washed three times with 1× PBS, and TRIzol was directly applied to cultures. In each case, we isolated RNA following the manufacturer's protocol, and quantified the total RNA. We synthesized double-stranded cDNA from 1.0 μg of RNA, using Random Hexamers (Applied Biosystems, Branchburg, NJ, USA) and Multiscribe Reverse Transcriptase (Applied Biosystems). cDNA was amplified using the TaqMan Universal PCR Master Mix (Applied Biosystems) with TaqMan gene expression–specific primers-probes (Applied Biosystems) for proteoglycan 4 (*Prg4*), PTH/PTH-related protein receptor (PPR), osteocalcin (OCN), collagen type II (col2), peroxisome proliferator-activated receptor-gamma2 (PPARγ2), insulin-like growth factor I (IGF-I), and basic fibroblast growth factor 2 (FGF-2). We used rodent glyceraldehyde-3-phosphate dehydrogenase (GAPDH) (Applied Biosystems) as an endogenous control. Amplification was performed using the ABI Prism 7700 Sequence Detection System (Applied Biosystems). Relative quantification of data was carried out using the standard curve method or the comparative CT method.[15]

Histomorphometry

Tibiae were fixed in 10% phosphate-buffered formalin for 48 hours at 4°C. We decalcified tibiae from young mice in 10% EDTA for 12 days at room temperature, and tibiae from adult mice in 10% EDTA for 21 days at room temperature. Proximal tibiae were embedded in paraffin, and 5 μm serial frontal sections were cut and stained. Hematoxylin and eosin (H&E) stain was performed in all proximal tibia sections. Growth plate height measurements were performed in H&E-stained proximal tibia sections from young mice. Five measurements of the proliferative zone and the hypertrophic zone were carried out in the central two-thirds of the growth plate of each sample as described by Yakar and colleagues.[16] Trabecular bone area (BA/TA) analysis was carried out in the secondary spongiosa of

H&E-stained proximal tibia sections from young and adult mice. Proximal tibia sections from adult mice were stained for tartrate resistant acid phosphatase (TRAP) using a commercial leukocyte acid phosphatase assay kit (Sigma-Aldrich). The number of TRAP+ multinucleated (three or more nuclei) cells per millimeter bone perimeter trabecular bone were quantified in the secondary spongiosa. Histomorphometric analysis of H&E-stained and TRAP-stained proximal tibia sections was performed using Image Pro Plus 5.1 software (Media Cybernetics, Silver Spring, MD, USA) interfaced with a Nikon Eclipse E800 light/epifluorescent microscope (Nikon Instruments, Melville, NY, USA).

We fixed tibiae from adult mice in 10% phosphate-buffered formalin for 48 hours at $4^{\circ}C$, dehydrated them in graded ethanols and xylene, and embedded them undecalcified in modified methylmethacrylate. Serial frontal proximal tibia sections (4 and 8 μm) were cut with vertical bed microtomes (Leica/Jung 2065 and 2165; Leica/Jung, Bannockburn, IL, USA) and affixed to slides precoated with 1% gelatin solution. Four-micrometer (4-μm) sections were stained by the von Kossa method with a tetrachrome counterstain (Polysciences, Warrington, PA, USA), and used for determining cellular endpoints. Eight-micrometer (8-μm) unstained sections were used for analyzing calcein labels. Bone histomorphometric data were collected semiautomatically with a Nikon Eclipse E800 light/epifluorescent microscope and the OsteoMeasure/Trabecular Analysis System (OsteoMetrics Inc., Atlanta, GA, USA).

We began analysis of methylmethacrylate-embedded proximal tibia sections 200 μm distal to the growth plate and 50 μm from the endocortical surfaces, including a 1200-μm (width) $\times$ 800-μm (length) area. The number of osteoblasts per bone perimeter (N.Ob/Pm) and osteoid surface (OS/BS) were assessed in von Kossa–stained (4-μm) sections. Fluorochrome (calcein)-based indices of bone formation including bone formation rate (BFR/BS), mineral apposition rate (MAR), and mineralizing surface (MS/BS) were analyzed in unstained (8-μm) sections. Bone histomorphometry data are reported in accordance with standardized nomenclature.[17]

Micro-CT

Femurs from young and adult mice were fixed in 10% phosphate-buffered formalin for 48 hours at $4^{\circ}C$, and stored them in 70% ethanol. Femurs were scanned in water at an 18-μm isotropic voxel resolution using eXplore Locus SP (GE Healthcare Pre-Clinical Imaging, London, ON, Canada), and calibrated three-dimensional images were reconstructed. Femur length was measured, and cortical bone morphology was assessed in a 1-mm segment of mid-diaphysis with GE Medical Systems MicroView v2.2 Advanced Bone Analysis Application software (GE Healthcare Pre-Clinical Imaging). The center plane of the 1-mm segment was defined as the midpoint between the most lateral point of the third trochanter and the most proximal point of the distal epiphyseal growth plate. Cortical bone morphometric variables analyzed included total area (Tt.Ar), cortical area (Ct.Ar), cortical area fraction (Ct.Ar/Tt.Ar), cortical thickness (Ct.Th), marrow area (Ma.Ar), endocortical perimeter (Ec.Pm), periosteal perimeter (Ps.Pm), and bone mineral density (BMD).

Femoral trabecular bone morphology and microarchitecture were analyzed using the stereology function of GE Medical Systems MicroView v2.2 Advanced Bone Analysis Application software. Transverse CT slices were analyzed beginning 360 μm proximal to the distal growth plate and extending 1.98 mm proximally. Trabecular bone morphometric variables analyzed included bone volume (BV/TV), trabecular number (Tb.N), trabecular thickness (Tb.Th), trabecular separation (Tb.Sp), and trabecular bone mineral density (Tb.BMD). Fixed thresholds of 1200 and 2000 Hounsfield Units for trabecular bone and cortical bone, respectively, were used to discriminate mineralized tissue. For samples from young mice, the location and length of the region of interest was adjusted in proportion to femoral length. Micro-CT data are reported in accordance with Bouxsein and colleagues.[18]

Bone marrow stromal cell in vitro assays

Femur and tibia whole bone marrow was isolated from untreated 16-week-old *Prg4* −/− and +/+ littermate mice. Epiphyses were sectioned, a 22G 0.5-inch needle was gently rotated into the marrow cavity, and marrow cells were flushed with α-modified minimum essential medium (α-MEM) (Invitrogen). Bone marrow cells were disassociated, cells counts performed, and cells plated at 3,000,000 cells/cm^2 in 60-mm dishes in α-MEM supplemented with 20% fetal bovine serum (FBS) (HyClone, Provo, UT, USA), 100 U/mL penicillin, 100 mg/mL streptomycin, 2 mM glutamine, and 10 nM dexamethasone (Sigma-Aldrich).

We isolated bone marrow stromal cells (BMSCs) (adherent cells) without passage at day 5. Culture media and nonadherent cells were aspirated, and BMSCs were washed, trypsinized, and plated in α-MEM supplemented with 10% FBS, 100 U/mL penicillin, 100 mg/mL streptomycin, 2 mM glutamine for assays. Plating cell density was assay dependent. Each in vitro assay was carried out at least 2 times.

In a cell-enumeration assay, we plated first-passage BMSCs in 24-well plates at 20,000 cells/cm^2. Cultures were carried out in triplicate and medium was changed every other day. Cell counting was performed on days 1, 3, 5, 7, and 9 using trypan blue dye and a hemacytometer.

We used a flow cytometry (FACS) bromodeoxyuridine (BRDU) cell proliferation assay and a FACS Annexin V cell apoptosis assay with first-passage BMSCs. BMSCs were plated at 20,000 cells/cm^2 in duplicate and medium was changed at day 2. At day 4, medium was aspirated and cells were washed with PBS. Cultures were trypsinized, proliferation assessed via an APC BRDU Flow Kit (BD Biosciences, San Jose, CA, USA), and apoptosis assessed using an FITC Annexin V Apoptosis Detection Kit I (BD Biosciences) according to the manufacturer's instructions. BRDU was administered to cultures 1 hour prior to harvest. Samples were analyzed using a FACS Calibur Flow Cytometer (BD Biosciences) and CellQuest Pro software (BD Biosciences).

In a von Kossa mineralization assay, we plated first-passage BMSCs in 12-well plates at 100,000 cells/cm^2. Cultures were carried out in triplicate and medium was changed every other day. Upon reaching confluency (day 4), cultures were treated with mineralization medium (50 μg/mL ascorbic acid, 10 mM β-glycerophosphate) for 14 days. At the end of the culture

period, cells were fixed with 95% EtOH and stained with 5% AgNO₃ using the von Kossa method to detect mineralization.[19] In another experimental protocol, upon reaching confluency (day 4) cultures were treated with mineralization medium and human PTH(1–34) (10 nM) (Bachem, Torrance, CA, USA) or vehicle (4 mM HCl/0.1% BSA) treatment every other day for 7 or 14 days. At the end of the culture period, cells were fixed and stained using the von Kossa method to detect mineralization.[19]

We used quantitative real-time PCR to evaluate genes associated with cell differentiation. First-passage BMSCs were plated in 12-well plates at 100,000 cells/cm² and cultures were carried out in duplicate; and medium was changed every other day. Upon reaching confluency (day 4), cultures were treated with mineralization medium (50 μg/mL ascorbic acid, 10 mM β-glycerophosphate) for 5 days. At the end of the culture period, cultures were harvested for osteocalcin mRNA expression analysis. In another experimental protocol, first-passage BMSCs were plated at 20,000 cells/cm². At day 4, cultures were harvested for collagen type II (col2) and PPARγ2 mRNA expression analysis.

Serum biochemical assays

We collected whole blood by cardiac puncture at euthanasia, coagulated it at room temperature for 30 minutes, centrifuged it, and isolated the serum. Serum was stored at −80°C until assayed. Enzyme immunoassays were used to measure the serum concentrations of tartrate-resistant acid phosphatase form 5b (TRAP5b) (Immunodiagnostic Systems, Fountain Hills, AZ, USA), propeptide of type I procollagen (P1NP) (Immunodiagnostic Systems), osteocalcin (OCN) (Biomedical Technologies, Stoughton, MA, USA), intact PTH (Immutopics, San Clemente, CA, USA), fibroblast growth factor-23 (FGF-23) (C-Term) (Immutopics), insulin-like growth factor I (IGF-I) (R&D Systems, Minneapolis, MN, USA), and basic fibroblast growth factor-2 (FGF-2) (R&D Systems). Serum calcium concentration was analyzed by a colorimetric assay (Pointe Scientific, Canton, MI, USA). Assays were performed according to the manufacturers' instructions.

Joint range of motion and animal mobility

We assessed joint range of motion by measuring maximal hind paw extension. Adult mice were anesthetized with isoflurane, the right tibia was immobilized at 0 degrees on a protractor, and maximal right hind paw extension was recorded.

We assessed animal mobility by monitoring spontaneous exploratory behavior. Adult mice were placed in a 30-cm × 40-cm chamber, divided into twelve 10-cm × 10-cm grids. Chamber walls were 10 cm in height, and constructed with a firm transparent plastic material. Mice were placed in the chamber and videotaped via a Flip Video HD camera (Cisco, San Jose, CA, USA) for 1 minute. Videos were reviewed to score the number of grids crossed and number of hindlimb stands. A hindlimb stand was enumerated when the animal braced its forepaws against the chamber wall and elevated its body with the hindpaws. The spontaneous exploratory behavior study was performed in the animal housing facility during the early morning (1:00–2:00 a.m.). Mice were directly transferred from their housed cage into the 12-grid chamber. The 12-grid chamber was set up in a laminar flow hood positioned within reaching distance of all housed cages to minimize stressing the mice prior to assessing spontaneous exploratory behavior.

Statistical analysis

We performed unpaired t tests using GraphPad Instat Software (GraphPad Software, San Diego, CA, USA). For comparison of +/+ PTH versus −/− PTH samples, values were expressed as treatment over control prior to statistical analysis. Data are presented as mean ± standard error of mean (SEM), and statistical significance is $p < 0.05$ or lower. Statistical analysis was carried out in consultation with the Center for Statistical Consultation and Research (CSAR) at the University of Michigan.

Results

PTH regulates *Prg4* mRNA in bone and liver

Quantitative real-time PCR studies assessing *Prg4* mRNA expression in long bone, calvaria, bone marrow, and whole liver from untreated 16-week-old C57BL6 mice showed that *Prg4* is expressed at highest levels in long bone and liver (Fig. 1A). Based on the high relative expression of *Prg4* mRNA in liver (Fig. 1A), and because the liver expresses PPR (Fig. 1B),[20,21] we assessed the impact of PTH on liver *Prg4* mRNA expression. A single subcutaneous injection of PTH(1–34) (1 μg/g) in 16-week-old C57BL6 wild-type mice significantly increased liver *Prg4* mRNA (fourfold) 4 hours after injection, and liver *Prg4* mRNA remained significantly upregulated 8 and 12 hours after injection (Fig. 1C). A single subcutaneous injection of PTH(1–34) also increased *Prg4* mRNA in calvaria and long bone (threefold) 4 hours after injection (Fig. 1D, E), showing that PTH regulates *Prg4* gene expression similarly in bone and liver. Whereas the biologic role of PPR expression in the liver is unclear, the liver has been shown to support skeletal homeostasis[16,22,23] and PTH anabolic actions in the skeleton.[24,25]

Decreased bone and blunted PTH anabolic actions in *Prg4* −/− mice

Histomorphometric analysis of trabecular bone area (BA/TA) in H&E-stained proximal tibia sections revealed marginally less trabecular BA/TA in young *Prg4* −/− mice versus +/+ littermates (Fig. 2A, B), whereas adult *Prg4* −/− mice had significantly decreased trabecular BA/TA relative to +/+ littermates (Fig. 2B, C). PTH similarly increased trabecular BA/TA in young *Prg4* +/+ and −/− mice, by 25% and 34%, respectively (Fig. 2A, B). PTH treatment induced an 82% increase in trabecular BA/TA in adult *Prg4* +/+ mice versus a 21% increase in −/− littermates ($p < 0.001$) (Fig. 2B, C), showing that PTH anabolic actions increasing trabecular BA/TA are blunted in adult *Prg4* −/− mice.

Results from the micro-CT analysis of trabecular bone volume (BV/TV) in the distal femur were similar to the histomorphometric analysis of proximal tibia. Young and adult *Prg4* −/− mice had significantly less trabecular BV/TV versus age-matched +/+ littermates (Fig. 2D–F). The increase in trabecular BV/TV by PTH was similar in young *Prg4* +/+ (130%) and −/− mice (149%) (Fig. 2D, E). PTH treatment resulted in an 89% increase in trabecular BV/TV in adult *Prg4* +/+ mice versus a 44% increase
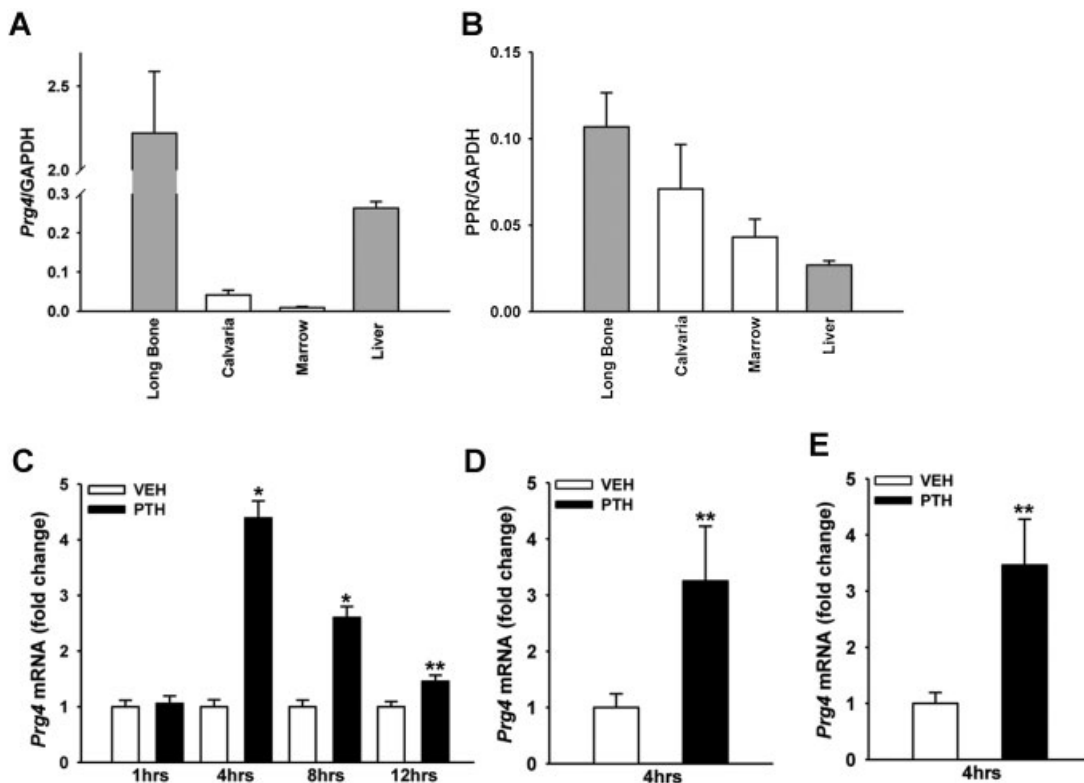
Fig. 1. PTH regulation of *Prg4* mRNA. (A, B) Untreated 16-week-old C57BL6 wild-type mice were euthanized, and long bone, calvaria, bone marrow, and liver were harvested for gene expression analysis ($n = 3$/group). RNA was isolated and quantitative real-time PCR was performed to assess; (A) proteoglycan 4 (*Prg4*) mRNA, and (B) PTH/PTHrP receptor (PPR) mRNA expression (standardized to GAPDH levels). Relative quantification of data was determined using the standard curve method. (C–E) Eight- to 16-week-old C57BL6 wild-type mice were administered a single subcutaneous injection of PTH(1–34) (1 μg/g) or vehicle (VEH) (0.9% NaCl) control, euthanized 1, 4, 8, or 12 hours later, and whole liver, calvaria, and long bone were harvested for gene expression analysis ($n \geq 5$/group). RNA was isolated and quantitative real-time PCR was performed to assess *Prg4* mRNA expression (standardized to GAPDH levels) in (C) liver, (D) calvaria, and (E) long bone. Relative quantification of data generated was carried out using the comparative CT method. $^*p < 0.001$; $^{**}p < 0.05$ versus time-matched VEH. Data are expressed as mean ± SEM.

in −/− littermates ($p \leq 0.10$) (Fig. 2E, F), revealing that PTH actions increasing trabecular BV/TV are marginally reduced in adult *Prg4* −/− mice.

Further analysis of trabecular bone parameters in the distal femur showed decreased trabecular bone mineral density (Tb.BMD), trabecular number (Tb.N), and increased trabecular separation (Tb.Sp) in both young and adult *Prg4* −/− mice (Table 1). Of interest, there was no difference in trabecular thickness (Tb.Th) in *Prg4* −/− versus +/+ mice. PTH increased Tb.BMD, Tb.Th, Tb.N, and decreased Tb.Sp similarly in young *Prg4* −/− versus +/+ mice. Interestingly, the anabolic actions of PTH increasing Tb.Th and Tb.BMD were significantly blunted in adult *Prg4* −/− versus +/+ mice. PTH induced a 39% increase in Tb.Th in adult *Prg4* +/+ mice versus a 13% increase in −/− mice ($p < 0.05$). Moreover, PTH treatment resulted in a 41% increase in Tb.BMD in adult *Prg4* +/+ mice versus a 16% increase in −/− mice ($p < 0.05$).

Micro-CT analysis of cortical bone in the femoral mid-shaft showed no difference in cortical area fraction (Ct.Ar/Tt.Ar), cortical thickness (Ct.Th), or cortical bone mineral density (BMD) in young *Prg4* −/− versus +/+ mice. Adult *Prg4* −/− mice had decreased Ct.Ar/Tt.Ar and Ct.Th versus +/+ littermates. Further analysis of cortical bone parameters revealed that adult *Prg4* −/− mice had increased cortical marrow area (Ma.Ar) and

marginally increased endocortical perimeter (Ec.Pm) relative to +/+ littermates. Whereas PTH increased Ct.Ar/Tt.Ar, Ct.Th, and BMD in adult *Prg4* +/+ mice, there was a lack of anabolic response to PTH in adult *Prg4* −/− mice (Table 1).

Altered growth plate in young *Prg4* −/− mice

We assessed growth-plate morphology and height in proximal tibiae from young *Prg4* −/− and +/+ mice to evaluate alterations in endochondral bone formation. The proliferative zone chondrocytes in *Prg4* −/− mice were arranged in short interrupted columns compared to long continuous columns in *Prg4* +/+ mice (Fig. 3A). Whereas the proliferative zone height was similar in *Prg4* −/− versus +/+ mice, the hypertrophic zone height and total growth plate height were reduced in *Prg4* −/− versus +/+ mice (Fig. 3B–D). PTH increased the hypertrophic zone height and total growth plate height similarly in *Prg4* −/− versus +/+ mice (Fig. 3C, D). Measurements of femur length showed no difference in longitudinal growth of long bones in young *Prg4* −/− versus +/+ mice (Fig. 3E).

Reduced biochemical markers of bone formation in young *Prg4* −/− mice

We used serum biochemical assays to investigate alterations in bone modeling and response to PTH in young *Prg4* −/− mice.
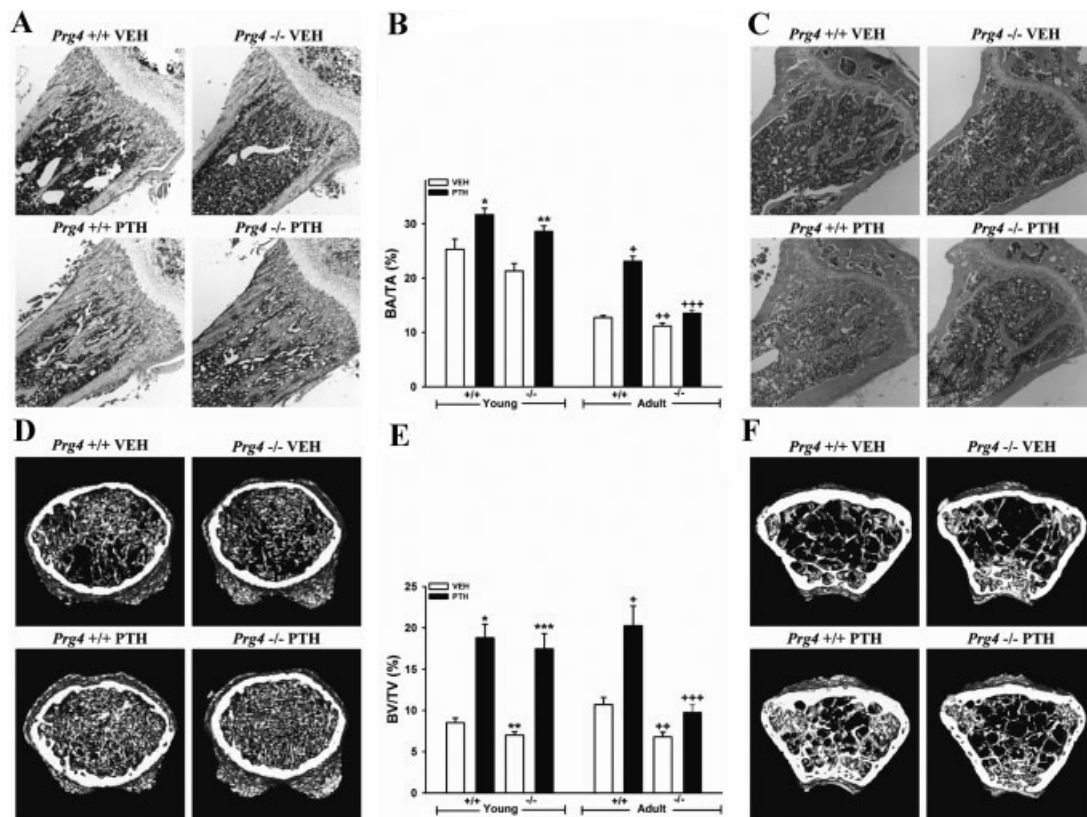
Fig. 2. Trabecular bone area and volume analysis. (A,B,D,E) Four-day-old *Prg4* mutant (−/−) and wild-type (+/+) mice were administered intermittent PTH(1–34) (50 μg/kg) or vehicle (VEH) (0.9% NaCl) subcutaneous injection daily for 17 days ("young" mice). (B,C,E,F) Sixteen-week-old *Prg4* −/− and +/+ mice were administered intermittent PTH(1–34) (50 μg/kg) or vehicle (VEH) (0.9% NaCl) control subcutaneous injection daily for 6 weeks ("adult" mice). Femur and tibia were harvested at time of euthanasia. (A–C) Histomorphometric analysis of trabecular bone area (BA/TA) in proximal tibia (secondary spongiosa) of young ($n \geq 11$/group) and adult ($n \geq 13$/group) mice. Representative images (4×) of H&E stained proximal tibial sections from, (A) young and (C) adult mice. (B) Trabecular BA/TA in the proximal tibia (secondary spongiosa). $^*p < 0.01$ versus +/+ VEH; $^{**}p < 0.001$ versus −/− VEH; $^+p < 0.001$ versus +/+ VEH; $^{++}p < 0.05$ versus +/+ VEH; $^{+++}p < 0.01$ versus −/− VEH and +/+ PTH. (D–F) Micro-CT analysis of distal femur trabecular bone volume fraction (BV/TV) in young ($n \geq 11$/group) and adult ($n = 8$/group) mice. Representative reconstructed micro-CT cross-sectional images of distal femur from (D) young and (F) adult mice. Representative images were captured in the distal femur, extending 0.5 mm proximally from where analysis was initiated. (E) Distal femur trabecular BV/TV. $^*p < 0.001$ versus +/+ VEH; $^{**}p < 0.05$ versus +/+ VEH; $^{***}p < 0.001$ versus −/− VEH; $^+p < 0.01$ versus +/+ VEH; $^{++}p < 0.01$ versus +/+ VEH; $^{+++}p < 0.05$ versus −/− VEH. For comparison of +/+ PTH versus −/− PTH samples, values were expressed as treatment over control prior to statistical analysis. Data are expressed as mean ± SEM.

Markers for bone formation, serum propeptide of type I procollagen (P1NP) and serum osteocalcin (OCN), were decreased in vehicle-treated *Prg4* −/− versus +/+ mice (Table 2). PTH did not alter serum P1NP in *Prg4* −/− or +/+ mice (Table 2). PTH increased serum OCN in *Prg4* −/− mice, but did not effect serum OCN in +/+ mice (Table 2). There was no difference in serum TRAP5b, a marker for bone resorption, in control *Prg4* mice, and PTH increased serum TRAP5b in *Prg4* −/− versus +/+ mice similarly (Table 2).

Lack of differences in *Prg4* −/− BMSCs

We performed BMSC in vitro assays to elucidate cell-intrinsic differences in *Prg4* −/− stromal/osteoblastic cells. There was no difference in *Prg4* −/− versus +/+ BMSC numbers over time (Fig. 4A), cell proliferation (Supplementary Fig. S1A), or cell apoptosis (Supplementary Fig. S1B). There was no difference in collagen type II (col2) and PPARγ2 mRNA expression in undifferentiated day 4 BMSC cultures (Fig. 4B, C), and OCN

mRNA expression was similar in day 9 differentiated BMSC cultures (Fig. 4D), which suggests that BMSCs from *Prg4* −/− mice do not have alterations in differentiation. Similar mineralization was present in day 7 and day 14 *Prg4* −/− versus +/+ BMSC cultures (Fig. 4E, F) (Supplementary Fig. S1C-F), which further suggests that BMSCs from *Prg4* −/− mice do not have intrinsic alterations in differentiation. Furthermore, PTH administration similarly decreased mineralization in day 7 and day 14 *Prg4* −/− versus +/+ BMSC cultures (Supplementary Fig. S1C–F), which shows that BMSCs from *Prg4* −/− and +/+ mice respond similarly to PTH at the cellular level.

Similar bone remodeling in adult *Prg4* −/− and +/+ mice

In order to elucidate whether differences in bone cell numbers or activity mediate the osteopenic skeletal phenotype and blunted anabolic response to PTH in adult *Prg4* −/− mice, we performed static cellular and dynamic histomorphometric analyses in the

Table 1. Femur Micro-CT Analysis

	+/+ VEH	+/+ PTH	−/− VEH	−/− PTH
Young *Prg4* mice (*n* ≥ 11/gp)				
Trabecular bone				
BV/TV (%)	8.50 ± 0.57	18.8 ± 1.64***	7.00 ± 0.39*	17.5 ± 1.83+++
Tb.Th (μm)	27.7 ± 0.64	36.5 ± 1.21***	26.6 ± 0.32	33.3 ± 1.55+++
Tb.Sp (μm)	309 ± 18.2	167 ± 11.5***	365 ± 19.0*	177 ± 20.0+++
Tb.N (mm^{-1})	3.04 ± 0.15	5.07 ± 0.29***	2.62 ± 0.13*	5.11 ± 0.38+++
Tb.BMD (mg/cc)	134 ± 3.54	191 ± 9.19***	123 ± 3.38*	187 ± 9.65+++
Cortical bone				
Tt.Ar (mm^2)	1.37 ± 0.07	1.32 ± 0.04	1.35 ± 0.04	1.26 ± 0.04
Ct.Ar (mm^2)	0.37 ± 0.03	0.33 ± 0.02	0.34 ± 0.01	0.31 ± 0.02
Ct.Ar/Tt.Ar (%)	26.6 ± 0.82	24.5 ± 1.02	25.2 ± 0.60	24.2 ± 0.98
Ct.Th (μm)	96.1 ± 5.43	86.2 ± 5.09	89.5 ± 3.05	83.3 ± 4.54
Ma.Ar (mm^2)	1.00 ± 0.04	0.99 ± 0.02	1.01 ± 0.03	0.96 ± 0.02
Ec.Pm (mm)	3.61 ± 0.08	3.61 ± 0.04	3.62 ± 0.05	3.53 ± 0.04
Ps.Pm (mm)	4.20 ± 0.11	4.14 ± 0.07	4.17 ± 0.06	4.05 ± 0.06
BMD (mg/cc)	235 ± 8.52	207 ± 10.5	219 ± 7.42	208 ± 9.01
Adult *Prg4* mice (*n* = 8/gp)				
Trabecular bone				
BV/TV (%)	10.7 ± 0.87	20.3 ± 2.40** (89%)	6.79 ± 0.57**	9.78 ± 0.90+ (44%)
Tb.Th (μm)	32.5 ± 0.61	45.0 ± 2.99** (39%)	29.9 ± 1.70	33.9 ± 1.50# (13%)
Tb.Sp (μm)	283 ± 21.9	188 ± 18.7** (−34%)	424 ± 29.9**	320 ± 24.5+ (−25%)
Tb.N (mm^{-1})	3.28 ± 0.23	4.49 ± 0.36* (37%)	2.26 ± 0.13**	2.88 ± 0.23+ (28%)
Tb.BMD (mg/cc)	197 ± 11.8	278 ± 19.3*** (41%)	168 ± 9.42*	184 ± 9.85+,# (16%)
Cortical bone				
Tt.Ar (mm^2)	1.74 ± 0.03	1.94 ± 0.05** (12%)	1.80 ± 0.03	1.88 ± 0.04# (4.1%)
Ct.Ar (mm^2)	0.88 ± 0.01	1.02 ± 0.02** (17%)	0.83 ± 0.02	0.86 ± 0.02## (3.7%)
Ct.Ar/Tt.Ar (%)	50.5 ± 0.66	52.7 ± 0.64* (4.2%)	46.1 ± 0.88**	45.9 ± 0.37## (−0.3%)
Ct.Th (μm)	221 ± 3.06	246 ± 3.15** (11%)	202 ± 5.34**	204 ± 3.52### (1.3%)
Ma.Ar (mm^2)	0.86 ± 0.02	0.92 ± 0.03 (7.2%)	0.97 ± 0.02**	1.02 ± 0.02 (4.4%)
Ec.Pm (mm)	3.50 ± 0.05	3.63 ± 0.07 (3.6%)	3.61 ± 0.03	3.69 ± 0.04 (2.1%)
Ps.Pm (mm)	4.89 ± 0.05	5.15 ± 0.09* (5.4%)	4.91 ± 0.06	4.97 ± 0.05 (1.3%)
BMD (mg/cc)	511 ± 9.46	562 ± 14.2** (10%)	483 ± 15.0	491 ± 6.14# (1.6%)

gp = group; VEH = vehicle; PTH = parathyroid hormone; BV/TV = bone volume; Tb.Th = trabecular thickness; Tb.Sp = trabecular separation; Tb.N = trabecular number; Tb.BMD = trabecular bone mineral density; Tt.Ar = total area; Ct.Ar = cortical area; Ct.Ar/Tt.Ar = cortical area fraction; Ct.Th = cortical thickness; Ma.Ar = marrow area; Ec.Pm = endocortical perimeter; Ps.Pm = periosteal perimeter; BMD = bone mineral density.

Data are expressed as mean ± SEM. Percentage increase over control analysis is presented in parenthesis.

*$p < 0.05$ versus +/+ VEH; **$p < 0.01$ versus +/+ VEH; ***$p < 0.001$ versus +/+ VEH; +$p < 0.05$ versus −/− VEH; ++$p < 0.01$ versus −/− VEH; +++$p < 0.001$ versus −/− VEH; #$p < 0.05$ versus +/+ PTH; ##$p < 0.01$ versus +/+ PTH, ###$p < 0.001$ versus +/+ PTH.

secondary spongiosa of proximal tibiae from adult *Prg4* mice (Fig. 5A–H). There were no differences in numbers of osteoblasts per bone perimeter (N.Ob/B.Pm), osteoclastic TRAP+ cells per bone perimeter, osteoid surface (OS/BS), bone formation rates (BFR/BS), or mineral apposition rates (MAR) in control *Prg4* −/− versus +/+ mice, and PTH increased N.Ob/B.Pm, TRAP+ cells, OS/BS, BFR/BS, and MAR in *Prg4* −/− versus +/+ mice similarly (Fig. 5A–H). These findings indicate that trabecular bone cell numbers, bone formation, and bone mineralization are unaffected by lack of proteoglycan 4 in the mature remodeling skeleton. Moreover, serum biochemical assays showed no differences in markers for bone turnover or mineral homeostasis in adult *Prg4* −/− mice (Supplementary Fig. S2).

Restricted joint range of motion and decreased mobility in adult *Prg4* −/− mice

Based on reports that adult *Prg4* −/− mice have failing articular joints[12] with significant loss of cartilage structure, stiffness, and frictional properties,[26] we investigated changes in the joints of *Prg4* −/− mice, which could contribute to the osteopenic skeletal phenotype and blunted PTH anabolic response in adult *Prg4* −/− mice. Maximal hind paw extension was assessed as a measure of joint range of motion (Fig. 6A, B), and spontaneous exploratory behavior was monitored to evaluate animal mobility (Fig. 6C, D). Maximal hind paw extension was limited to 115 degrees in *Prg4* −/− mice compared to 170 degrees in +/+ mice (Fig. 6A, B). The scoring of spontaneous exploratory behavior in a
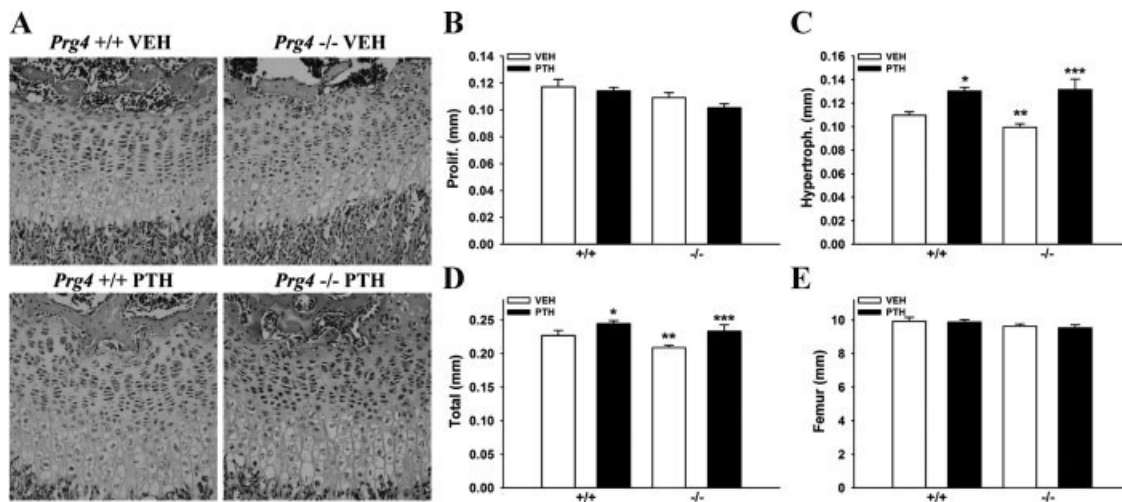
Fig. 3. Tibial growth plate and femur length analysis in young mice. (A–E) Four-day-old *Prg4* mutant (−/−) and wild-type (+/+) mice were administered intermittent PTH(1–34) (50 μg/kg) or vehicle (VEH) (0.9% NaCl) control subcutaneous injection daily for 17 days ("young" mice). (A–D) Tibial growth plate morphology and height were evaluated in H&E-stained proximal tibia sections from young *Prg4* −/− versus +/+ mice ($n \geq 11$/group). (A) Representative images (40 ×) of tibial growth plate from young *Prg4* −/− versus +/+ mice. (B) Proliferative zone height. (C) Hypertrophic zone height. *$p < 0.001$: versus +/+ VEH; **$p < 0.05$: versus +/+ VEH; ***$p < 0.01$: versus −/− VEH. (D) Total growth plate height. *$p < 0.05$: versus +/+ VEH; **$p < 0.05$: versus +/+ VEH; ***$p < 0.05$: versus −/− VEH. (E) Femur length measurements performed via reconstructed micro-CT images of young *Prg4* femurs ($n \geq 11$/group).

12-grid chamber showed that *Prg4* −/− mice crossed fewer grids and stood on their hindlimbs fewer times than +/+ littermates (Fig. 6C, D) (Supplementary Video S3A,B). Because the adult *Prg4* −/− mice do not display gross signs of muscle weakness, pain, or neurological deficits it is likely that that the reduced animal mobility is attributed to compromised joint structure and function[12,26] (Fig. 6A, B). The decreased joint range of motion and animal mobility showed by adult *Prg4* −/− mice suggests that skeletal loading is altered in *Prg4* −/− mice.

Reduced liver IGF-I and FGF-2 and marrow FGF-2 mRNA normalized by PTH in *Prg4* −/− mice

We isolated bone marrow and whole liver from adult *Prg4* mice to assess basal gene expression and the impact of 6 weeks daily PTH treatment on PPR, IGF-I, and FGF-2 mRNA expression. Marrow PPR mRNA was similar in control adult *Prg4* −/− and +/+ mice (Table 3), which suggests that similar numbers of PPR expressing osteoblastic cells are present in the marrow of adult *Prg4* −/− and +/+ mice. Liver PPR mRNA was decreased in control adult *Prg4* −/− versus +/+ mice (Table 3). It has been

reported that hepatocytes are the predominant PPR-expressing cells in the liver.[21]

We assessed IGF-I mRNA expression in marrow and liver because marrow-derived IGF-I and liver-derived IGF-I have been shown to independently support skeletal homeostasis[16,22,23] and PTH skeletal anabolism.[24,25] Stromal/osteoblastic cells express IGF-I locally in the bone marrow mediating autocrine/paracrine signaling,[27,28] and the liver secretes IGF-I into the circulation facilitating endocrine signaling in bone.[29]

Unexpectedly, PTH significantly decreased marrow IGF-I mRNA in adult *Prg4* +/+ mice and marginally decreased marrow IGF-I mRNA in adult *Prg4* −/− mice (Table 3). Although it has been reported that intermittent PTH increases IGF-I mRNA expression in bone matrix devoid of bone marrow,[5,30] we are unaware of prior studies that measured the effect of intermittent PTH on marrow IGF-I mRNA. Adult *Prg4* −/− mice had reduced liver IGF-I mRNA, and PTH normalized liver IGF-I mRNA in *Prg4* −/− mice to +/+ levels (Table 3). The decreased liver IGF-I mRNA in control adult *Prg4* −/− mice suggests that liver *Prg4* may be important for IGF-I expression in the liver.

We assessed FGF-2 mRNA as another critical regulator of skeletal remodeling[31] and PTH anabolic actions.[8,32] Adult *Prg4*

Table 2. Serum Biochemical Analyses

	+/+ VEH	+/+ PTH	−/− VEH	−/− PTH
Young *Prg4* mice ($n = 9$/gp)				
P1NP (ng/mL)	584.32 ± 43.50	580.41 ± 30.44	377.30 ± 35.64**	388.13 ± 35.31
OCN (ng/mL)	190.11 ± 21.23	213.98 ± 20.30	135.21 ± 15.16*	295.40 ± 47.62++
TRAP5b (U/L)	18.52 ± 2.06	24.30 ± 1.13*	15.09 ± 1.51	21.19 ± 1.61+

Data are expressed as mean ± SEM.
gp = group; VEH = vehicle; PTH = parathyroid hormone.
*$p < 0.05$ versus +/+ VEH; **$p < 0.01$ versus +/+ VEH; +$p < 0.05$ versus −/− VEH; ++$p < 0.01$ versus −/− VEH.
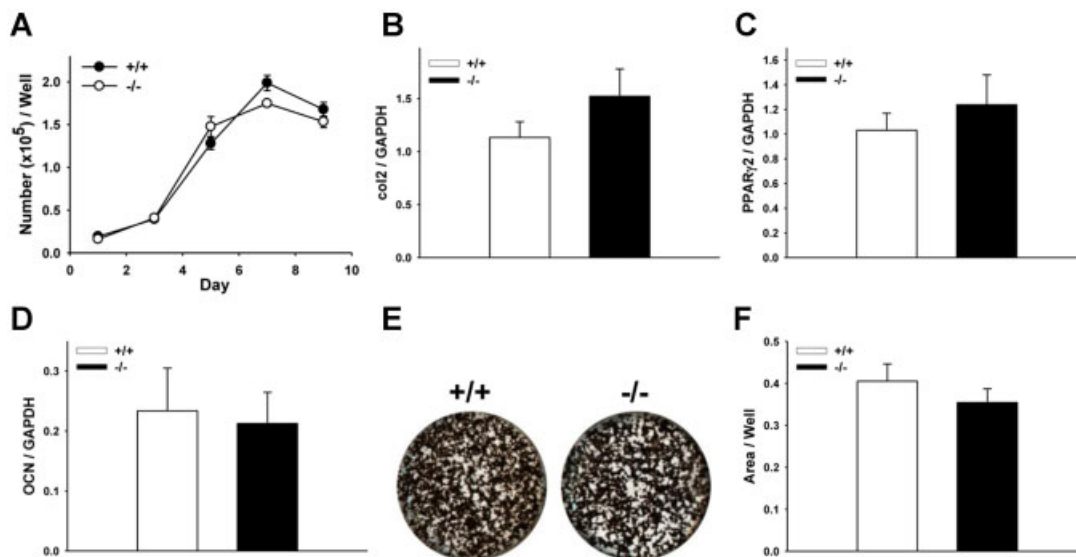
Fig. 4. Bone marrow stromal cell (BMSC) in vitro osteoblastogenesis assays. (*A–F*) Untreated 16-week-old *Prg4* mutant (−/−) and wild-type (+/+) mice were euthanized, femoral and tibial bone marrow was harvested, and BMSCs were isolated for in vitro osteoblastogenesis assays. (*A*) Cell numbers over time in BMSC cultures ($n \geq 6$/group). (*B*) Collagen type II (col2) mRNA expression was assessed as a marker of chondrogenic potential in day 4 BMSC cultures ($n \geq 6$/group). (*C*) Peroxisome proliferator-activated receptor-gamma2 (PPARγ2) mRNA expression was assessed as a marker of adipogenic potential in day 4 BMSC cultures ($n \geq 6$/group). (*D*) Osteocalcin (OCN) mRNA expression was assessed as a marker of osteoblast differentiation in day 9 BMSC cultures ($n \geq 10$/group). RNA was standardized to GAPDH levels and relative quantification of data generated was determined using the standard curve method. (*E*) Representative images of day 14 BMSC von Kossa mineralization cultures. (*F*) Mineralization area per well in day 14 BMSC cultures ($n \geq 6$/group). In vitro assays were carried out at least two times with similar results. Data are expressed as mean ± SEM.

−/− mice had lower marrow and liver FGF-2 mRNA than +/+ mice (Table 3), which implies that *Prg4* supports FGF-2 gene expression in marrow and liver. PTH increased marrow and liver FGF-2 mRNA in adult *Prg4* −/− mice to +/+ levels (Table 3).

Reduced serum FGF-2 normalized by PTH in *Prg4* −/− mice

We assayed serum IGF-I and FGF-2 in adult *Prg4* −/− and +/+ mice to determine if alterations in *Prg4* −/− marrow and liver mRNA expression resulted in changes in the concentration of circulating proteins. There was no difference in serum IGF-I in adult *Prg4* −/− and +/+ mice (Table 4), which suggests that the reduced liver IGF-I mRNA expression in *Prg4* −/− mice is sufficient to support normal levels of circulating IGF-I. In contrast, adult *Prg4* −/− mice had lower serum FGF-2 levels, and PTH increased serum FGF-2 in *Prg4* −/− mice to +/+ levels (Table 4). The reduced serum FGF-2 correlated with decreased liver and marrow FGF-2 mRNA in adult *Prg4* −/− mice, which were normalized to +/+ levels by PTH. Whereas circulating IGF-I has been shown to be secreted primarily by the liver (75% to 80%),[29] the source of circulating FGF-2 is unclear. Based on quantitative real-time PCR showing comparable FGF-2 mRNA expression in bone marrow and liver (data not shown), we speculate that decreased circulating FGF-2 levels in adult *Prg4* −/− mice are attributed to both decreased marrow and liver FGF-2 mRNA expression.

PTH alters gene expression similarly in bone marrow and liver

Because PTH regulates *Prg4* mRNA expression similarly in bone and liver (Fig. 1*C–E*), we used single PTH injection studies to elucidate whether *Prg4* regulates the expression of several critical PTH-responsive osteogenic genes in bone and liver. PTH decreased marrow PPR mRNA at 1 hour and increased marrow PPR mRNA 8 hours after injection similarly in 16-week-old *Prg4* −/− and +/+ mice (Fig. 7*A*). PTH decreased liver PPR mRNA 4 hours after injection similarly in *Prg4* −/− and +/+ mice (Fig. 7*D*). The finding that PTH similarly downregulates PPR mRNA in bone marrow and liver suggests that proteoglycan 4 does not modify PTH binding and signaling at the PPR receptor in bone or liver.

Although intermittent PTH treatment has been reported to increase IGF-I mRNA expression in bone matrix in vivo,[5,30] little is known regarding the temporal effects of PTH on IGF-I mRNA expression. Marrow IGF-I mRNA was decreased 4 hours after PTH injection in *Prg4* +/+ mice. Twelve hours following PTH injection, marrow IGF-I mRNA was significantly increased in *Prg4* +/+ mice. PTH did not significantly alter marrow IGF-I mRNA in *Prg4* −/− or liver IGF-1 mRNA expression in *Prg4* −/− or +/+ mice (Fig. 7*B, E*).

Single PTH injection significantly increased marrow and liver FGF-2 mRNA in *Prg4* −/− and +/+ mice at 1 hour (Fig. 7*C, F*). These findings were consistent with prior studies that showed FGF-2 is an early immediate PTH-responsive gene in bone.[4]

Consistent with control adult *Prg4* −/− mice (Table 3), control 16-week-old *Prg4* −/− mice (Fig. 7*A, B*) had similar marrow PPR and IGF-I mRNA levels compared to age-matched +/+ mice. Whereas control adult *Prg4* −/− mice had decreased marrow FGF-2 mRNA (Table 3), marrow FGF-2 mRNA was similar in control 16-week-old *Prg4* −/− versus +/+ mice (Fig. 7*C*). This finding indicates that decreased marrow FGF-2 mRNA in adult *Prg4* −/− mice is likely secondary to changes with age in the adult *Prg4* −/− mice. Although there are no known studies
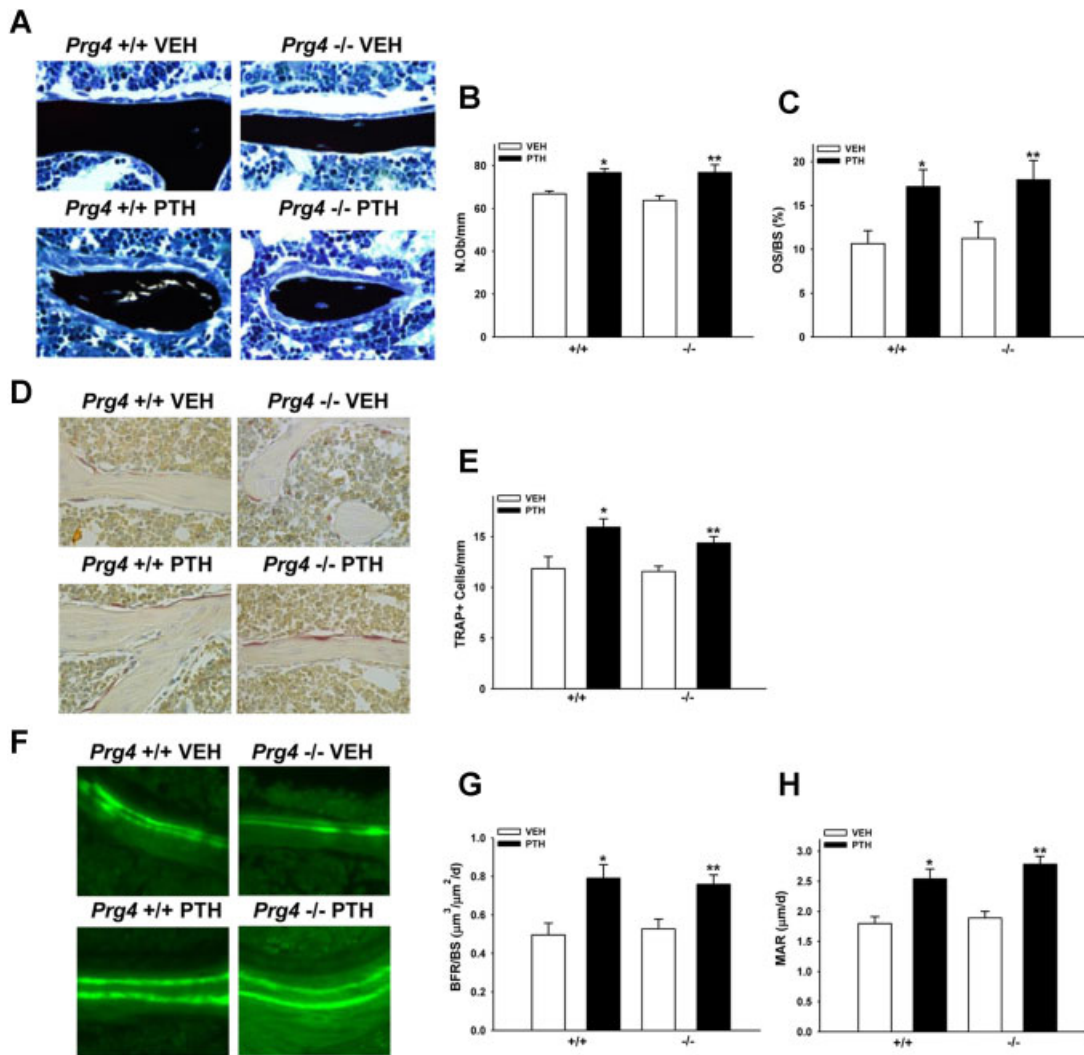
Fig. 5. Proximal tibia bone cell numbers and activity. (A–H) Sixteen-week-old *Prg4* mutant (−/−) and wild-type (+/+) mice were administered intermittent PTH(1–34) (50 μg/kg) or vehicle (VEH) (0.9% NaCl) control subcutaneous injection daily for 6 weeks ("adult" mice). Tibiae were isolated from adult *Prg4* −/− and +/+ mice for histomorphometric analysis of bone cell numbers and activity. (A–C) Histomorphometric analysis of von Kossa–stained (with tetrachrome counterstain) proximal tibia sections was performed to assess osteoblast number per bone perimeter (N.Ob/B.Pm) and osteoid surface (OS/BS) in the secondary spongiosa. (A) Representative images (40 ×) of von Kossa–stained proximal tibia secondary spongiosa. (B) Osteoblast numbers ($n \geq 10$/group). $^*p < 0.001$ versus +/+ VEH; $^{**}p < 0.01$ versus −/− VEH. (C) Osteoid surface ($n \geq 10$/group). $^*p < 0.05$ versus +/+ VEH; $^{**}p < 0.05$ versus −/− VEH. (D,E) TRAP+ cell enumeration was carried out in proximal tibia sections to assess osteoclast numbers per bone perimeter in the secondary spongiosa. (D) Representative images (40 ×) of TRAP-stained proximal tibia secondary spongiosa. (E) TRAP+ cell number per bone perimeter ($n \geq 8$/group). $^*p < 0.05$ versus +/+ VEH; $^{**}p < 0.01$ versus −/− VEH. (F–H) Dynamic histomorphometric analysis of calcein-labeled proximal tibia sections was performed to assess bone formation rates (BFR/BS) and mineral apposition rates (MAR) in the secondary spongiosa. (F) Representative images (40 ×) of dual calcein labels in proximal tibia secondary spongiosa. (G) Bone formation rate ($n \geq 8$/group). $^*p < 0.01$ versus +/+ VEH; $^{**}p < 0.01$ versus −/− VEH. (H) Mineral apposition rate ($n \geq 8$/group). $^*p < 0.01$ versus +/+ VEH; $^{**}p < 0.01$ versus −/− VEH. Data are expressed as mean ± SEM.

reporting the impact of skeletal loading/unloading on FGF-2 mRNA expression in bone, it is possible that altered skeletal loading in *Prg4* mutant mice may secondarily mediate the decreased marrow FGF-2 mRNA.

Similar to control adult *Prg4* −/− mice (Table 3), control 16-week-old *Prg4* −/− mice (Fig. 7D–F) had decreased liver PPR, IGF-I, and FGF-2 mRNA versus age-matched control +/+ mice. These consistent gene expression findings in the liver of adult *Prg4* −/− mice and 16-week-old *Prg4* −/− mice indicate that liver *Prg4* supports physiologic PPR, IGF-I, and FGF-2 gene expression in the liver.

Discussion

The four *Prg4* protein products—lubricin, superficial zone protein (SZP), hemangiopoietin (HAPO), and megakaryocyte stimulating factor (MSF)—are secreted glycoproteins that have been implicated in the protection of articular joints, support of hematopoietic progenitor cells, and regulation of megakaryopoiesis. Although studies report that proteoglycan 4 has diverse biologic actions, proteoglycan 4 receptors have not been identified and receptor sites are unknown.[12,13] Although most studies of *Prg4* have focused on the role of the *Prg4* gene product
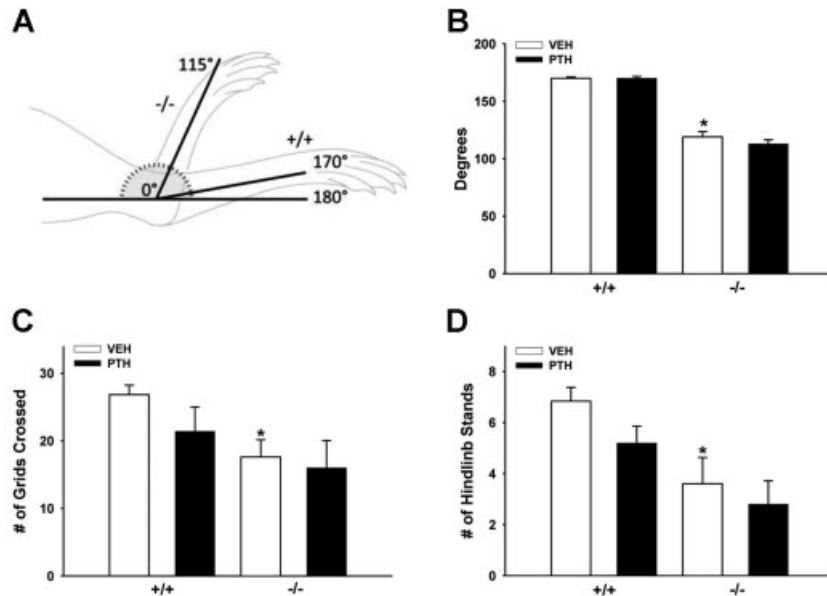
Fig. 6. Joint range of motion and animal mobility. (A–D) Sixteen-week-old *Prg4* mutant (−−) and wild-type (+/+) mice were administered intermittent PTH(1–34) (50 μg/kg) or vehicle (VEH) (0.9% NaCl) control subcutaneous injection daily for 6 weeks ("adult" mice). (A,B) Maximal hind paw extension was measured to assess joint range of motion. (A) Tibia was immobilized at 0 degrees and the maximal extension of the hind paw was measured. (B) Maximal hind paw extension ($n \geq 5$/group). *$p < 0.001$ versus +/+ VEH. (C,D) Spontaneous exploratory behavior was assessed to evaluate animal mobility. Mice were placed in a 12-grid chamber for 1 minute; parameters assessed included number of grids crossed and number of hindlimb stands. (C) Number of grids crossed ($n \geq 5$/group). *$p < 0.01$ versus +/+ VEH. (D) Number of hindlimb stands ($n \geq 5$/group). *$p < 0.05$ versus +/+ VEH. Data are expressed as mean ± SEM.

lubricin and joint function, we hypothesized that proteoglycan 4 also plays a role in skeletal development and remodeling based upon *Prg4* expression in bone[11] and the noted osteopenic phenotype in the *Prg4* mutant mouse.[12] Furthermore, our findings that *Prg4* is a PTH-responsive gene in bone[10] lead us to speculate that proteoglycan 4 supports the anabolic actions of PTH in the skeleton.

Lubricin and SZP are expressed locally in the synovial joints by synoviocytes and superficial zone articular chondrocytes, having lubricating and protective effects.[12,33] Whereas the source of

Table 3. Real-Time PCR Analysis: Bone Marrow and Liver mRNA

	+/+ VEH	+/+ PTH	−/− VEH	−/− PTH
Adult *Prg4* mice ($n = 4$–5/gp)				
Marrow mRNA				
PPR	1.00 ± 0.19	0.84 ± 0.06	0.77 ± 0.08	0.64 ± 0.05
IGF-I	1.00 ± 0.03	0.80 ± 0.05*	0.89 ± 0.09	0.68 ± 0.04
FGF-2	1.00 ± 0.08	1.01 ± 0.05	0.68 ± 0.06*	0.91 ± 0.08+
Liver mRNA				
PPR	1.00 ± 0.08	0.98 ± 0.14	0.68 ± 0.06*	0.86 ± 0.09
IGF-I	1.00 ± 0.14	1.02 ± 0.13	0.59 ± 0.06*	1.03 ± 0.07++
FGF-2	1.00 ± 0.14	1.17 ± 0.16	0.63 ± 0.04*	1.21 ± 0.11++

gp = group; PPR = PTH/PTHrP receptor; IGF-I = insulin-like growth factor I; FGF-2 = basic fibroblast growth factor 2. mRNA expression was standardized to GAPDH levels, and relative quantification of data generated was carried out using the comparative CT method. Data are expressed as mean ± SEM.
*$p < 0.05$ versus +/+ VEH; +$p < 0.05$ versus −/− VEH,
++$p < 0.01$ versus −/− VEH.

HAPO and MSF is unknown, based on studies that implicate HAPO and MSF in the regulation of hematopoiesis[13,34] and demonstration of high *Prg4* expression in liver and bone[11] (major sites of hematopoiesis), it is likely that both liver and bone act as considerable sources of proteoglycan 4. The novel finding that *Prg4* is a PTH-responsive gene not only in bone but also liver implies that both marrow- and liver-derived proteoglycan 4 are candidate regulators of skeletal remodeling and the anabolic actions of PTH.

The finding that young *Prg4* mutant mice have decreased trabecular bone suggests that proteoglycan 4 plays a role in endochondral bone formation. The decreased height of the growth plate hypertrophic zone in young *Prg4* mutant mice suggests that proteoglycan 4 regulates growth plate chondrocyte maturation,[35] which could have implications for endochondral cartilage ossification in developing long bone. Similar femoral length in young *Prg4* mutant and wild-type mice indicates that abnormalities in the growth plates of *Prg4* mutant mice do not impact long bone longitudinal growth.

Although there were reduced numbers of trabeculae and increased trabecular separation in both young and adult *Prg4* mutant versus wild-type mice, there was no difference in trabecular thickness. This suggests that proteoglycan 4 functions to support the formation of distinct trabeculae during endochondral bone formation, but does not effect the remodeling of trabeculae. Based upon the findings that serum P1NP and OCN were decreased, and there were no differences in cortical bone or serum TRAP5b in young *Prg4* mutant mice, we speculate that the reduced number of trabeculae is associated with decreased bone formation in young *Prg4* mutant mice.

Table 4. Serum Biochemical Analysis: IGF-I and FGF-2

Adult *Prg4* mice	+/+ VEH	+/+ PTH	−/− VEH	−/− PTH
Serum protein				
IGF-I (ng/mL) ($n = 4$–5/gp)	603.19 ± 28.78	589.78 ± 7.38	538.29 ± 32.52	554.81 ± 24.79
FGF-2 (pg/mL) ($n = 5$–6/gp)	4.00 ± 0.76	3.82 ± 1.13	1.07 ± 0.30**	5.32 ± 1.12++

gp = group; IGF-I = insulin-like growth factor I; FGF-2 = basic fibroblast growth factor 2. Data are expressed as mean ± SEM.
**$p < 0.01$ versus +/+ VEH; ++$p < 0.01$ versus −/− VEH.

Because BMSCs from *Prg4* mutant mice were normal, proteoglycan 4 actions supporting osteoblast-mediated formation of trabeculae appear to be unique to the process of endochondral bone formation. The lack of difference in bone cell numbers or activity in the secondary spongiosa of adult *Prg4* mutant mice shows that proteoglycan 4 is not a critical regulator of skeletal remodeling at trabecular sites in the mature skeleton. This finding suggests that the trabecular bone osteopenic phenotype in adult *Prg4* mutant mice is likely secondary to proteoglycan 4 actions supporting endochondral bone formation.

Based on studies characterizing the role of FGF-2 in skeletal development and remodeling, we speculate that the decreased marrow and serum FGF-2 levels may play a role in the trabecular bone osteopenia in *Prg4* mutant mice. Exogenous FGF-2 administration stimulates endosteal and endochondral bone formation in growing rats.[36] In adult rats, FGF-2 stimulates bone formation at endosteal and trabecular bone surfaces,[37,38] and has been shown to induce the formation of de novo bone spicules within the marrow cavity.[37] FGF-2 is expressed in differentiating growth plate chondrocytes, the centers of ossification, and the calcified matrix,[39] which suggests that FGF-2 plays a role in the formation of trabeculae during endochondral bone formation. Bone marrow stromal/osteoblastic cells secrete FGF-2[40,41] that signals to stromal/osteoblastic cells in an autocrine/paracrine manner.[42,43] Whereas the liver expresses FGF-2,[44,45] little is known regarding the role of the liver in secreting FGF-2 into the circulation, or the impact of circulating FGF-2 on the skeleton. Findings in the present study suggest that liver-derived FGF-2 contributes to circulating levels which impact skeletogenesis.

Similarities in the skeleton of *Prg4* mutant and FGF-2 mutant mice suggest that FGF-2 is a candidate regulator of proteoglycan
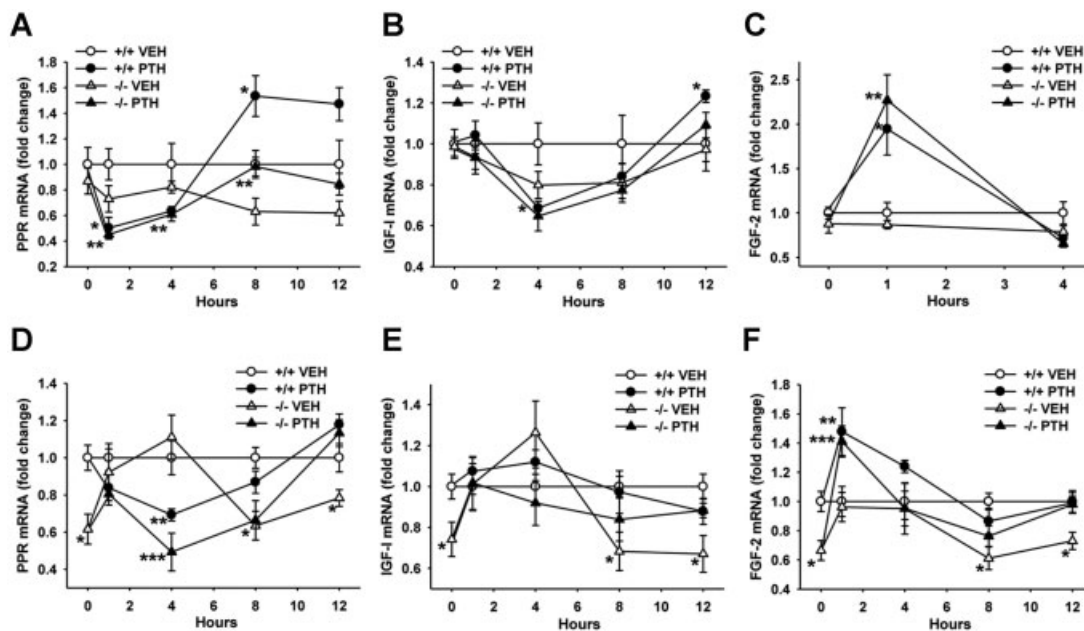

Fig. 7. PTH regulation of bone marrow and liver gene expression. (A–F) Sixteen-week-old *Prg4* mutant (−/−) and wild-type (+/+) mice were administered a single subcutaneous injection of PTH(1–34) (1 μg/g) or vehicle (VEH) (0.9% NaCl) control, euthanized 0 (no treatment control), 1, 4, 8, or 12 hours later, and long bone marrow ($n \geq 5$/group) and whole liver ($n \geq 5$/group) harvested for gene expression analysis. RNA was isolated and quantitative real-time PCR was performed to assess marrow; (A) PTH/PTHrP receptor (PPR), (B) insulin-like growth factor I (IGF-I), (C) basic fibroblast growth factor 2 (FGF-2), and liver; (D) PPR, (E) IGF-I, (F) FGF-2 mRNA expression (standardized to GAPDH levels). Relative quantification of data was determined using the comparative CT method. Line graphs represent PTH effects on mRNA expression over time. (A) Marrow PPR mRNA; *$p < 0.05$: +/+ PTH versus +/+ VEH; **$p < 0.05$: −/− PTH versus −/− VEH. (B) Marrow IGF mRNA; *$p < 0.05$: +/+ PTH versus +/+ VEH. (C) Marrow FGF-2 mRNA; *$p < 0.05$: +/+ PTH versus +/+ VEH; **$p < 0.01$: −/− PTH versus −/− VEH. (D) Liver PPR mRNA; *$p < 0.05$: −/− VEH versus +/+ VEH; **$p < 0.05$: +/+ PTH versus +/+ VEH; ***$p < 0.01$: −/− PTH versus −/− VEH. (E) Liver IGF-I mRNA; *$p < 0.05$: −/− VEH versus +/+ VEH. (F) Liver FGF-2 mRNA; *$p < 0.05$: −/− VEH versus +/+ VEH; **$p < 0.05$: +/+ PTH versus +/+ VEH; ***$p < 0.05$: −/− PTH versus −/− VEH. Data are expressed as mean ± SEM.

4 actions supporting the formation of numbers of trabeculae. Whereas neither *Prg4* mutant or FGF-2 mutant mice exhibit gross abnormalities in skeletal development or remodeling, both models have significantly reduced trabecular bone in the proximal tibia and distal femur sites that becomes more severe with age.[31] Uniquely similar to the young and adult *Prg4* mutant mice, 18-week-old FGF-2 mutant mice have decreased numbers of trabeculae with increased trabecular separation, but no difference in trabecular thickness.[31]

Although there are no known studies investigating the osteogenic role of circulating FGF-2, based on studies showing that circulating IGF-I has osteogenic effects separate from marrow IGF-I,[16,22–25] we speculate that circulating FGF-2 may have an important role in skeletal homeostasis and PTH skeletal anabolism. Similar to the actions of PTH increasing serum FGF-2 levels in the osteopenic *Prg4* mutant mice, intermittent PTH has been reported to increase serum FGF-2 levels in osteoporotic patients.[46] These data imply that the anabolic actions of PTH in the osteopenic/osteoporotic skeleton are mediated at least in part by an increase in circulating FGF-2.

Based on studies showing that exogenous FGF-2 does not increase periosteal bone formation[36,47] and FGF-2 mutant mice do not have reported abnormalities in cortical bone,[31] it does not appear that the osteopenia of cortical bone in *Prg4* mutant mice is caused by the reduced FGF-2 levels. Because there were no differences in cortical bone in the femur of young *Prg4* mutant mice, the finding that cortical area fraction and cortical thickness were decreased in the femur of adult *Prg4* mutant mice indicates that proteoglycan 4 supports cortical bone homeostasis in the mature remodeling skeleton. The increased endocortical perimeter and marrow area associated with the decreased cortical bone thickness in the femur of adult *Prg4* mutant mice suggests that endocortical resorption is occurring at a more rapid rate than periosteal bone formation. Taking into consideration that adult *Prg4* mutant mice had decreased joint range of motion and animal mobility, it is likely that altered skeletal loading may account for the cortical bone osteopenic phenotype. Similar to the cortical bone osteopenia in adult *Prg4* mutant mice, rodent hindlimb immobilization studies have shown that cortical bone disuse osteopenia is characterized by decreased cortical thickness, increased endocortical perimeter, and expansion of the marrow cavity.[48,49] Although we have proposed that the trabecular bone osteopenia in adult *Prg4* mutant mice is likely secondary to altered endochondral bone formation, it is possible that altered skeletal loading may contribute to the decreased trabecular bone in adult *Prg4* mutant mice.

Although there have been controversial findings from investigations of PTH anabolic actions in rodent hindlimb immobilization models, studies showing that loading is a critical regulator of PTH actions increasing trabecular and cortical bone[50,51] imply that the blunted PTH-induced increase in bone in adult *Prg4* mutant mice may be a result of compromised joint function leading to altered skeletal loading. PTH has been reported to restore lost trabecular bone in unloaded rats to the levels of nontreated loaded controls,[50,51] which is similar to what was seen in the present study in which PTH-treated adult *Prg4* mutant mice had similar trabecular bone levels as untreated wild-type mice. Similar to the lack of a PTH increase in cortical bone in adult *Prg4* mutant mice, PTH does not significantly prevent cortical bone loss or restore lost cortical bone in unloaded rats compared to the levels of nontreated loaded controls.[50,52]

It is perplexing and not totally clear why adult *Prg4* mutant mice have a normal PTH anabolic response at the cellular level (PTH increase in trabecular bone osteoblast numbers, osteoid surface, osteoclast numbers, bone formation rate, and mineral apposition rate) yet a blunted PTH anabolic response at the tissue level (PTH increase in trabecular bone area and volume). Rodent hindlimb immobilization studies of trabecular bone disuse osteopenia have reported an acute phase, characterized by increased bone resorption and decreased bone formation, and a chronic phase during which bone cells re-equilibrate and bone remodeling returns to physiologic levels.[53–55] Taking into consideration that joint structure and function is significantly disrupted in *Prg4* mutant mice by 16 weeks of age,[12,26] which appears to alter skeletal loading, we speculate that adult *Prg4* mutant mice have a blunted tissue-level response to PTH due a transient disruption of bone cell numbers and actions (acute phase), which resolved by 22 weeks of age (chronic phase).

Whereas there have been reports suggesting that the anabolic actions of PTH on trabecular bone are independent of the level of mechanical usage,[56,57] findings from the current study of blunted PTH actions on trabecular bone in the compromised joint status of the *Prg4* mutant mice suggest that biomechanical impact is a critical regulator of PTH anabolic actions. This study of the effects of PTH in an animal model having precocious joint failure raises the question of the efficacy of PTH anabolic therapy in patients afflicted by arthropathic joint conditions that alter skeletal loading.

The novel finding that PTH regulates PPR, FGF-2, and *Prg4* mRNA expression similarly in bone and liver suggests that the liver plays an important role in mediating the biologic actions of PTH. Historically, PTH research has focused on the role of bone as a mediator of PTH biologic actions. This focus is well grounded in knowledge that stromal/osteoblastic cells are the predominant cells in the body expressing the PPR, and PTH signaling in stromal/osteoblastic cells regulates the local expression of factors critical for the anabolic actions of PTH. In conjunction with studies showing that the anabolic actions of PTH are blunted in hepatocyte-specific IGF-I knockout models,[24,25] the present study and work by Mitnick and colleagues,[58] which show that PTH regulates liver gene and protein expression, emphasize the need for investigations of the role of the liver as a mediator of PTH biologic actions.

This original investigation of *Prg4* actions in the skeleton revealed that proteoglycan 4 is an important regulator of skeletal development, remodeling, and PTH anabolic actions. Proteoglycan 4 supports endochondral bone formation and the attainment of peak trabecular bone mass in the developing skeleton. In the mature remodeling skeleton, proteoglycan 4 appears to indirectly support skeletal homeostasis and PTH anabolic actions by protecting joint function. Bone- and liver-derived FGF-2 are candidate regulators of proteoglycan 4 actions supporting the formation of trabeculae numbers. In summary, proteoglycan 4 is a dynamic factor supporting skeletogenesis and PTH

skeletal anabolism via actions regulating trabecular bone formation and protecting joint biomechanics. Finally, in addition to well-characterized actions in osteoblasts, PTH likely impacts skeletogenesis via actions in the liver.

Disclosures

All authors state that they have no conflicts of interest.

Acknowledgments

References

1. Kousteni S, Bilezikian JP. Cellular actions of parathyroid hormone. In: Bilezikian JP, Raisz LG, Martin TJ, editors. Principles of bone biology. 3rd ed. Burlington, MA: Elsevier Press; 2008. p. 639–56.

2. Aspenberg P, Genant HK, Johansson T, Nino AJ, See K, Krohn K, Garcia-Hernandez PA, Recknor CP, Einhorn TA, Dalsky GP, Mitlak BH, Fierlinger A, Lakshmanan MC. Teriparatide for acceleration of fracture repair in humans: a prospective, randomized, double-blind study of 102 postmenopausal women with distal radial fractures. J Bone Miner Res. 2010;25:404–14.

3. Bashutski JD, Eber RM, Kinney JS, Benavides E, Maitra S, Braun TM, Giannobile WV, McCauley LK. Teriparatide and osseous regeneration in the oral cavity. N Eng J Med. 2010;363:2396–405.

4. Hurley MM, Tetradis S, Huang YF, Hock J, Kream BE, Raisz LG. Parathyroid hormone regulates the expression of fibroblast growth factor-2 mRNA and fibroblast growth factor receptor mRNA in osteoblastic cells. J Bone Miner Res. 1999;14:776–83.

5. Watson P, Lazowski D, Han V, Fraher L, Steer B, Hodsman A. Parathyroid hormone restores bone mass and enhances osteoblast insulin-like growth factor 1 gene expression in ovariectomized rats. Bone. 1995;16:357–65.

6. Bikle DD, Sakata T, Leary C, Elalieh H, Ginzinger D, Rosen CJ, Beamer WG, Majumdar S, Halloran BP. Insulin-like growth factor I is required for the anabolic actions of parathyroid hormone on mouse bone. J Bone Miner Res. 2002;17:1570–8.

7. Miyakoshi N, Kasukawa Y, Linkhart TA, Baylink DJ, Mohan S. Evidence that anabolic effects of PTH on bone require IGF-1 in growing mice. Endocrinology. 2001;142:4349–56.

8. Hurley MM, Okada Y, Xiao L, Tanaka Y, Ito M, Okimoto N, Nakamura T, Rosen CJ, Doetschman T, Coffin JD. Impaired bone anabolic response to parathyroid hormone in Fgf2−/− and Fgf2+/− mice. Biochem Biophys Res Commun. 2006;341:989–94.

9. Novince CM, Koh AJ, Marchesan JT, McCauley LK. Proteoglycan-4: a novel gene regulating parathyroid hormone actions in bone anabolism and hematopoiesis. ASBMR Annual Meeting,

10. Novince CM, Koh AJ, Michalski MN, Marchesan JT, Wang J, Jung Y, Berry JE, Eber MR, Rosol TJ, Taichman RS, McCauley LK. Proteoglycan-4, a novel immunomodulatory factor, regulates parathyroid hormone actions on hematopoietic cells. Am J Pathol. 2011; Epub ahead of print. PMID: 21939632.

11. Ikegawa S, Sano M, Koshizuka Y, Nakamura Y. Isolation, characterization and mapping of the mouse and human PRG4 (proteoglycan 4) genes. Cytogenet Genome Res. 2000;90:291–7.

12. Rhee DK, Marcelino J, Baker M, Gong Y, Smits P, Lefebvre V, Jay GD, Stewart M, Wang H, Warman ML, Carpten JD. The secreted glycoprotein lubricin protects cartilage surfaces and inhibits synovial cell overgrowth. J Clin Invest. 2005;115:622–31.

13. Liu YJ, Lu SH, Xu B, Yang RC, Ren Q, Liu B, Li B, Lu M, Yan FY, Han ZB, Han ZC. Hemangiopoietin, a novel human growth factor for the primitive cells of both hematopoietic and endothelial cell lineages. Blood. 2004;103:4449–56.

14. Marcelino J, Carpten JD, Suwairi WM, Gutierrez OM, Schwartz S, Robbins C, Sood R, Makalowska I, Baxevanis A, Johnstone B, Laxer RM, Zemel L, Kim CA, Herd JK, Ihle J, Williams C, Johnson M, Raman V, Alonso LG, Brunoni D, Gerstein A, Papadopoulos N, Bahabri SA, Trent JM, Warman ML. CACP, encoding a secreted proteoglycan, is mutated in camptodactyly-arthropathy-coxa vara-pericarditis syndrome. Nat Genet. 1999;23:319–22.

15. Schmittgen TD, Livak KJ. Analyzing real-time PCR data by the comparative CT method. Nat Protoc. 2008;3:1101–8.

16. Yakar S, Rosen CJ, Beamer WG, Ackert-Bicknell CL, Wu Y, Liu JL, Ooi GT, Setser J, Frystyk J, Boisclair YR, Leroith D. Circulating levels of IGF-1 directly regulate bone growth and density. J Clin Invest. 2002;110:771–81.

17. Parfitt AM, Drezner MK, Glorieux FH, Kanis JA, Malluche H, Meunier PJ, Ott SM, Recker RR. Bone histomorphometry: standardization of nomenclature, symbols and units (Report of the ASBMR Histomorphometry Nomenclature Committee). J Bone Miner Res. 1987; 2:595–610.

18. Bouxsein ML, Boyd SK, Christiansen BA, Guldberg RE, Jepsen KJ, Muller R. Guidelines for assessment of bone microstructure in rodents using micro-computed tomography. J Bone Miner Res. 2010;25:1468–86.

19. Koh AJ, Beecher CA, Rosol TJ, McCauley LK. Cyclic AMP activation in osteoblastic cells: effects on PTH-1 receptors and osteoblastic differentiation in vitro. Endocrinology. 1999;140:3154–62.

20. Tian J, Smogorezewski M, Kedes L, Massry SG. Parathyroid hormone-parathyroid hormone related protein receptor messenger RNA is present in many tissues besides the kidney. Am J Nephrol. 1993; 13:210–3.

21. Watson PH, Fraher LJ, Hendy GN, Chung UI, Kisiel M, Natale BV, Hodsman AB. Nuclear localization of the type 1 PTH/PTHrP receptor in rat tissues. J Bone Miner Res. 2000;15:1033–44.

22. Sjögren K, Sheng M, Moverare S, Liu JL, Wallenius K, Tornell J, Isaksson O, Jansson JO, Mohan S, Ohlsson C. Effects of liver-derived insulin-like growth factor I on bone metabolism in mice. J Bone Miner Res. 2002;17:1977–87.

23. Elis S, Courtland HW, Wu Y, Rosen CJ, Sun H, Jepsen KJ, Majeska RJ, Yakar S. Elevated serum levels of IGF-1 are sufficient to establish normal body size and skeletal properties even in the absence of tissue IGF-1. J Bone Miner Res. 2010;25:1257–66.

24. Yakar S, Bouxsein ML, Canalis E, Sun H, Glatt V, Gundberg C, Cohen P, Hwang D, Boisclair Y, Leroith D, Rosen CJ. The ternary IGF complex influences postnatal bone acquisition and the skeletal response to intermittent parathyroid hormone. J Endocrinol. 2006; 189:289–99.

25. Elis S, Courtland HW, Wu J, Fritton JC, Sun H, Rosen CJ, Yakar S. Elevated serum IGF-1 levels synergize PTH action on the skeleton only when the tissue IGF-1 axis is intact. J Bone Miner Res. 2010; 25:2051–8.

26. Coles JM, Zhang L, Blum JJ, Warman ML, Jay GD, Guilak F, Zauscher S. Loss of cartilage structure, stiffness, and frictional properties in mice lacking PRG4. Arthritis Rheum. 2010;62:1666–74.

27. Linkhart TA, Mohan S. Parathyroid hormone stimulates release of insulin-like growth factor-I (IGF-I) and IGF-II from neonatal mouse calvaria in organ culture. Endocrinology. 1989;125:1484–91.

28. Lazowski DA, Fraher LJ, Hodsman A, Steer B, Modrowski D, Han VK. Regional variation of insulin-like growth factor-I gene expression in mature rat bone and cartilage. Bone. 1994;15:563–76.

29. Sjögren K, Liu JL, Blad K, Skrtic S, Vidal O, Wallenius V, Leroith D, Tornell J, Isaksson OG, Jansson JO, Ohlsson C. Liver-derived insulin-like growth factor I (IGF-I) is the principal source of IGF-I in blood but is not required for postnatal body growth in mice. Proc Natl Acad Sci U S A. 1999;96:7088–92.

30. Pfeilschifter J, Laukhuf F, Muller-Beckmann B, Blum WF, Pfister T, Ziegler R. Parathyroid hormone increases the concentration of insulin-like growth factor-I and transforming growth factor beta 1 in rat bone. J Clin Invest. 1995;96:767–74.

31. Montero A, Okada Y, Tomita M, Ito M, Tsurukami H, Nakamura T, Doetschman T, Coffin JD, Hurley MM. Disruption of the fibroblast growth factor-2 gene results in decreased bone mass and bone formation. J Clin Invest. 2000;105:1085–93.

32. Sabbieti MG, Agas D, Xiao L, Marchetti L, Coffin JD, Doetschman T, Hurley MM. Endogenous FGF-2 is critically important in PTH anabolic effects on bone. J Cell Physiol. 2009;219:143–51.

33. Schumacher BL, Hughes CE, Kuettner KE, Caterson B, Aydelotte MB. Immunodetection and partial cDNA sequence of the proteoglycan, superficial zone protein, synthesized by cells lining synovial joints. J Orthop Res. 1999;17:110–20.

34. Merberg DM, Fitz L, Temple P, Giannotti J, Murtha P, Fitzgerald M, Scaltreto H, Kelleher K, Preissner K, Kriz R, Jacobs K, Turner K. A comparison of vitronectin and megakaryocyte stimulating factor. In: Preissner KT, Kost C, Wegerhoff J, Mosher DF, editors. *Biology of vitronectins and their receptors*. Philadelphia: Elsevier; 1992. p. 45–53.

35. Kobayashi T, Chung UI, Schipani E, Starbuck M, Karsenty G, Katagiri T, Goad DL, Lanske B, Kronenberg HM. PTHrP and Indian hedgehog control differentiation of growth plate chondrocytes at multiple steps. Development. 2002;129:2977–86.

36. Nagai H, Tsukuda R, Mayahara H. Effects of basic fibroblast growth factor (bFGF) on bone formation in growing rats. Bone. 1995;16: 367–73.

37. Liang H, Pun S, Wronski TJ. Bone anabolic effects of basic fibroblast growth factor in ovariectomized rats. Endocrinology. 1999;140: 5780–8.

38. Nakamura T, Hanada K, Tamura M, Shibanushi T, Nigi H, Tagawa M, Fukumoto S, Matsumoto T. Stimulation of endosteal bone formation by systemic injections of recombinant basic fibroblast growth factor in rats. Endocrinology. 1995;136:1276–84.

39. Gonzalez AM, Buscaglia M, Ong M, Baird A. Distribution of basic fibroblast growth factor in the 18-day rat fetus: localization in the basement membranes of diverse tissues. J Cell Biol. 1990;110:753–65.

40. Brunner G, Gabrilove J, Rifkin DB, Wilson EL. Phospholipase C release of basic fibroblast growth factor from human bone marrow cultures as a biologically active complex with a phosphatidylinositol-anchored heparan sulfate proteoglycan. J Cell Biol. 1991;114: 1275–83.

41. Brunner G, Nguyen H, Gabrilove J, Rifkin DB, Wilson EL. Basic fibroblast growth factor expression in human bone marrow and peripheral blood cells. Blood. 1993;81:631–8.

42. Thomson BM, Bennett J, Dean V, Triffitt J, Meikle MC, Loveridge N. Preliminary characterization of porcine bone marrow stromal cells: skeletogenic potential, colony-forming activity, and response to dexamethasone, transforming growth factor beta, and basic fibroblast growth factor. J Bone Miner Res. 1993;8:1173–83.

43. Long MW, Robinson JA, Ashcraft EA, Mann KG. Regulation of human bone marrow-derived osteoprogenitor cells by osteogenic growth factors. J Clin Invest. 1995;95:881–7.

44. Chow NH, Cheng KS, Lin PW, Chan SH, Su WC, Sun YN, Lin XZ. Expression of fibroblast growth factor-1 and fibroblast growth factor-2 in normal liver and hepatocellular carcinoma. Digest Dis Sci. 1998;43:2261–6.

45. Hioki O, Minemura M, Shimizu Y, Kasii Y, Nishimori H, Takahara T, Higuchi K, Yoshitake Y, Nishikawa K, Watanabe A. Expression and localization of basic fibroblast growth factor (bFGF) in the repair process of rat liver injury. J Hepatol. 1996;24:217–24.

46. Hurley MM, Yao M, Lane NE. Changes in serum fibroblast growth factor 2 in patients with glucocorticoid-induced osteoporosis treated with human parathyroid hormone (1–34). Osteoporosis Int. 2005;16: 2080–4.

47. Mayahara H, Ito T, Nagai H, Miyajima H, Tsukuda R, Taketomi S, Mizoguchi J. Kat. In vivo stimulation of endosteal bone formation by basic fibroblast growth factor in rats. Growth Factors. 1993;9:73–80.

48. Bagi CM, Mecham M, Weiss J, Miller SC. Comparative morphometric changes in rat cortical bone following ovariectomy and/or immobilization. Bone. 1993;14:877–83.

49. Li XJ, Jee WS. Adaptation of diaphyseal structure to aging and decreased mechanical loading in the adult rat: a densitometric and histomorphometric study. Anat Rec. 1991;229:291–7.

50. Turner RT, Lotinun S, Hefferan TE, Morey-Holton E. Disuse in adult male rats attenuates the bone anabolic response to a therapeutic dose of parathyroid hormone. J Appl Physiol. 2006;101:881–6.

51. Halloran BP, Bikle DD, Haris J, Tanner S, Curren T, Morey-Holton E. Regional responsiveness of the tibia to intermittent administration of parathyroid hormone as affected by skeletal unloading. J Bone Miner Res. 1997;12:1068–74.

52. Moriyama I, Iwamoto J, Takeda T, Toyama Y. Comparative effects of intermittent administration of human parathyroid hormone (1–34) on cancellous and cortical bone loss in tail-suspended and sciatic neurectomized young rats. J Orthop Sci. 2002;7:379–85.

53. Li XJ, Jee WS, Chow SY, Woodbury DM. Adaptation of cancellous bone to aging and immobilization in the rat: a single photon absorptiometry and histomorphometry study. Anat Rec. 1990;227: 12–24.

54. Chen MM, Jee WS, Ke HZ, Lin BY, Li QN, Li XJ. Adaptation of cancellous bone to aging and immobilization in growing rats. Anat Rec. 1992; 234:317–34.

55. Li M, Jee WS, Ke HZ, Liang XG, Lin BY, Ma YF, Setterberg RB. Prostaglandin E2 restores cancellous bone to immobilized limb and adds bone to overloaded limb in right hindlimb immobilization rats. Bone. 1993;14:283–8.

56. Ma YF, Jee WS, Ke HZ, Lin BY, Liang XG, Li M, Yamamoto N. Human parathyroid hormone-(1–38) restores cancellous bone to the immobilized, osteopenic proximal tibial metaphysis in rats. J Bone Miner Res. 1995;10:496–505.

57. Turner RT, Evans GL, Cavolina JM, Halloran B, Morey-Holton E. Programmed administration of parathyroid hormone increases bone formation and reduces bone loss in hindlimb-unloaded ovariectomized rats. Endocrinology. 1998;139:4086–91.

58. Mitnick MA, Grey A, Masiukiewicz U, Bartkiewicz M, Rios-Velez L, Friedman S, Xu L, Horowitz MC, Insogna K. Parathyroid hormone induces hepatic production of bioactive interleukin-6 and its soluble receptor. Am J Physiol Endocrinol Metab. 2001;280:E405–12.